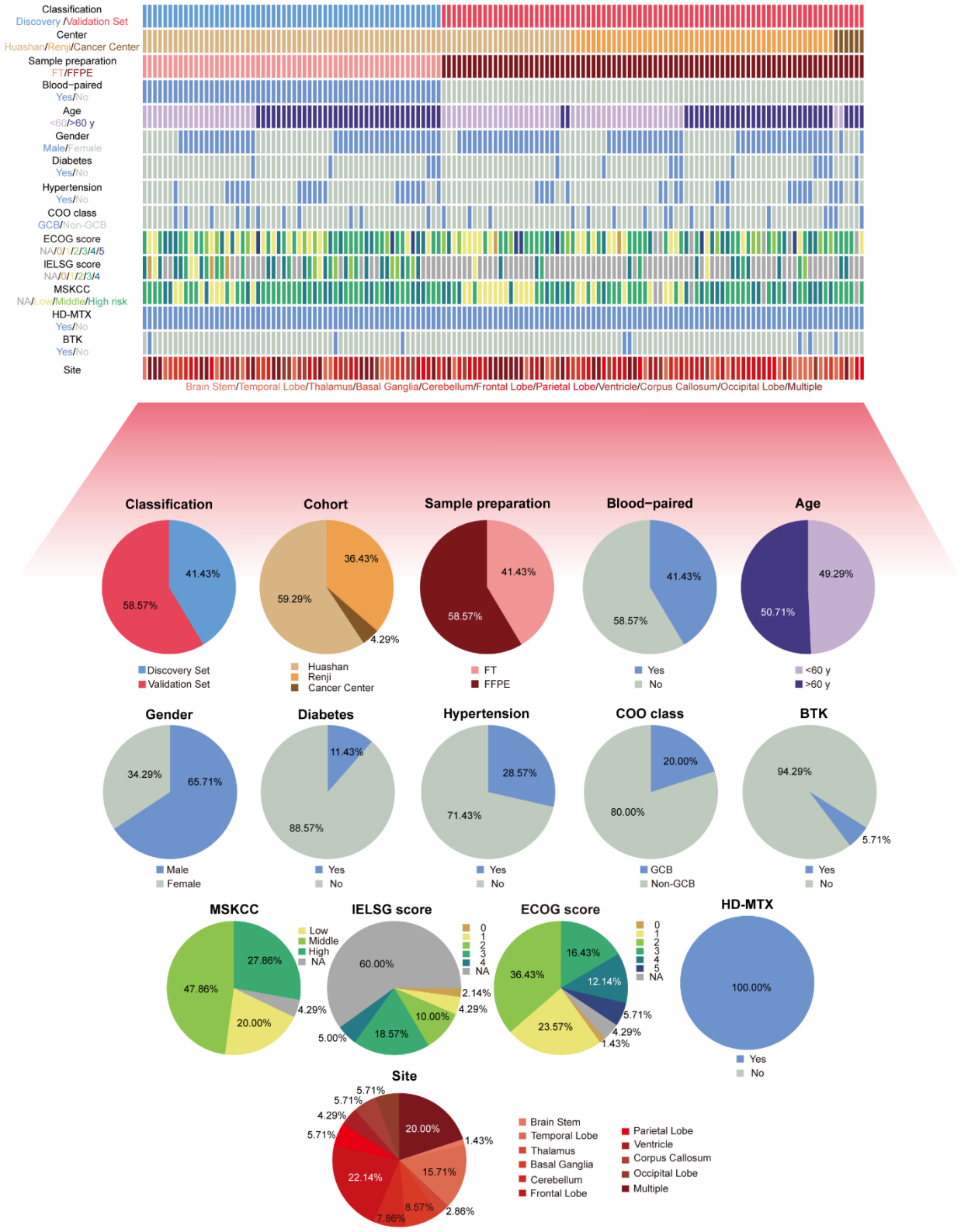

Figure S1. Basic information of the 140 PCNSL patients

The key demographic and clinical characteristics of PCNSL patients are summarized in the upper half of the figure, while the proportions of patients with these characteristics are presented in the lower half. Related to Figure 1.

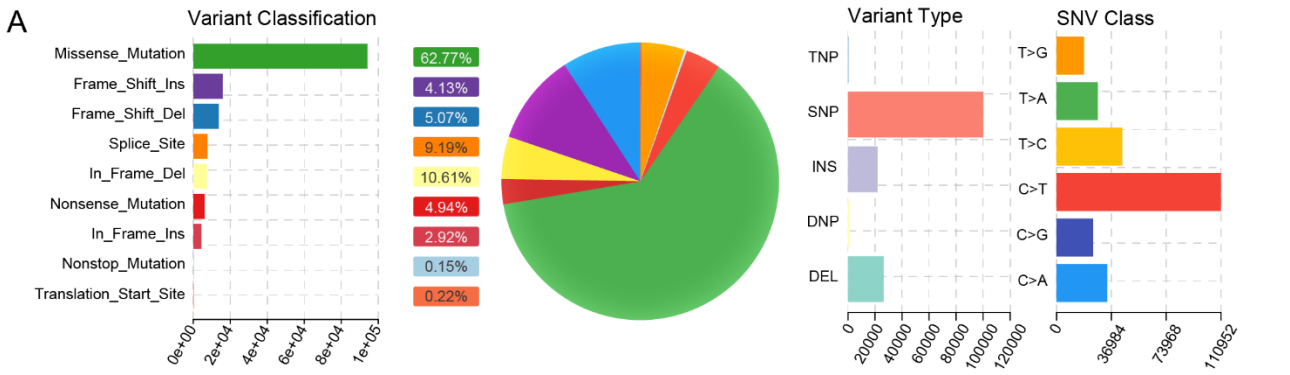
A
Variant Classification
Missense_Mutation
Frame_Shift_Ins
Frame_Shift_Del
Splice_Site
In_Frame_Del
Nonsense_Mutation
In_Frame_Ins
Nonstop_Mutation
Translation_Start_Site
62.77%
4.13%
5.07%
9.19%
10.61%
4.94%
2.92%
0.15%
0.22%
0e+00
2e+04
4e+04
6e+04
8e+04
1e+05
Variant Type
TNP
SNP
INS
DNP
DEL
0
20000
40000
60000
80000
100000
120000
SNV Class
T>G
T>A
T>C
C>T
C>G
C>A
0
36984
73968
110952

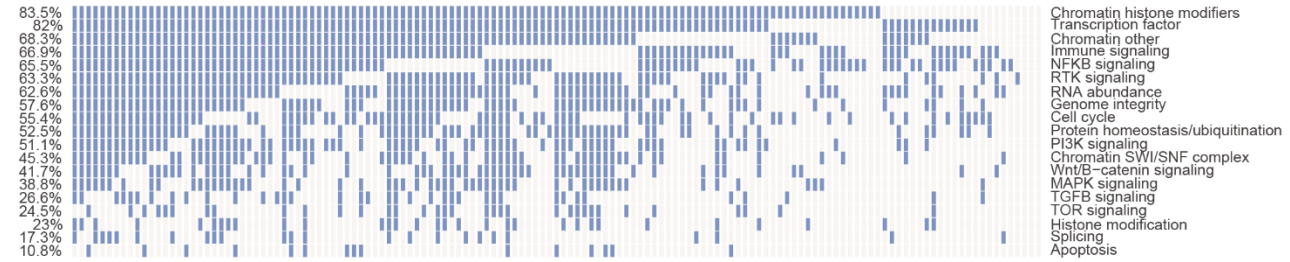
B
83.5%
82%
68.3%
66.9%
65.5%
63.3%
62.6%
57.6%
55.4%
52.5%
51.1%
45.3%
41.7%
38.8%
26.6%
24.5%
23%
17.3%
10.8%
Chromatin histone modifiers
Transcription factor
Chromatin other
Immune signaling
NFKB signaling
RTK signaling
RNA abundance
Genome integrity
Cell cycle
Protein homeostasis/ubiquitination
PI3K signaling
Chromatin SWI/SNF complex
Wnt/B−catenin signaling
MAPK signaling
TGFB signaling
TOR signaling
Histone modification
Splicing
Apoptosis

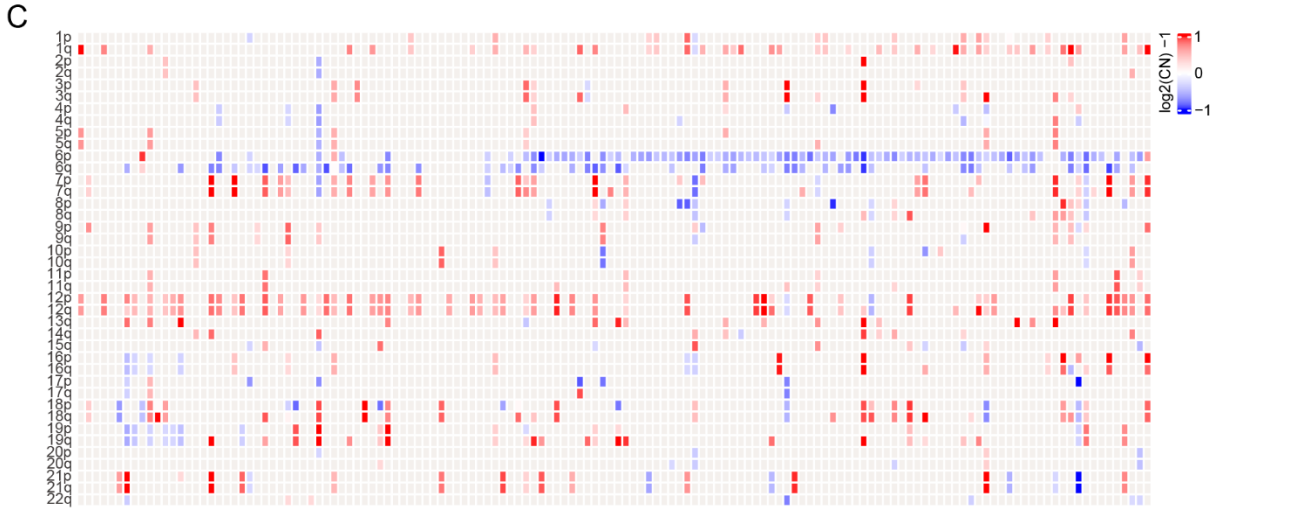
C
log2(CN)
1
0
−1

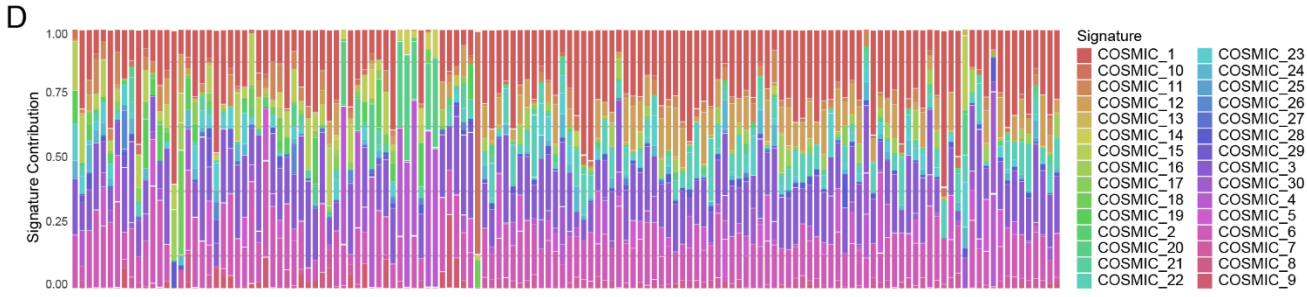
D
Signature Contribution
1.00
0.75
0.50
0.25
0.00
Signature
COSMIC_1
COSMIC_10
COSMIC_11
COSMIC_12
COSMIC_13
COSMIC_14
COSMIC_15
COSMIC_16
COSMIC_17
COSMIC_18
COSMIC_19
COSMIC_2
COSMIC_20
COSMIC_21
COSMIC_22
COSMIC_23
COSMIC_24
COSMIC_25
COSMIC_26
COSMIC_27
COSMIC_28
COSMIC_29
COSMIC_3
COSMIC_30
COSMIC_4
COSMIC_5
COSMIC_6
COSMIC_7
COSMIC_8
COSMIC_9

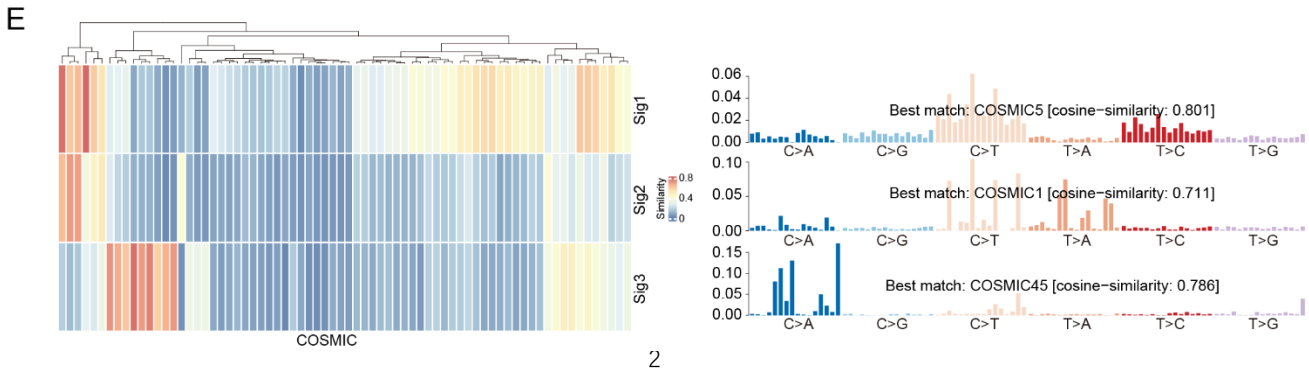
E
Sig1
Sig2
Sig3
Similarity
0.8
0.4
0
COSMIC
Best match: COSMIC5 [cosine−similarity: 0.801]
Best match: COSMIC1 [cosine−similarity: 0.711]
Best match: COSMIC45 [cosine−similarity: 0.786]
C>A
C>G
C>T
T>A
T>C
T>G

Figure S2. PCNSL mutational landscape and variation signature

A: Variant classification, type, and single-nucleotide variation class for PCNSL patients (n = 140).

B: Oncogene pathways in 140 PCNSL patients.

C: Arm-level copy number alterations in 140 PCNSL patients.

D: Contribution of mutational signatures in 140 PCNSL patients.

E: The most significant contributions to the PCNSL genome.

Related to Figure 1.

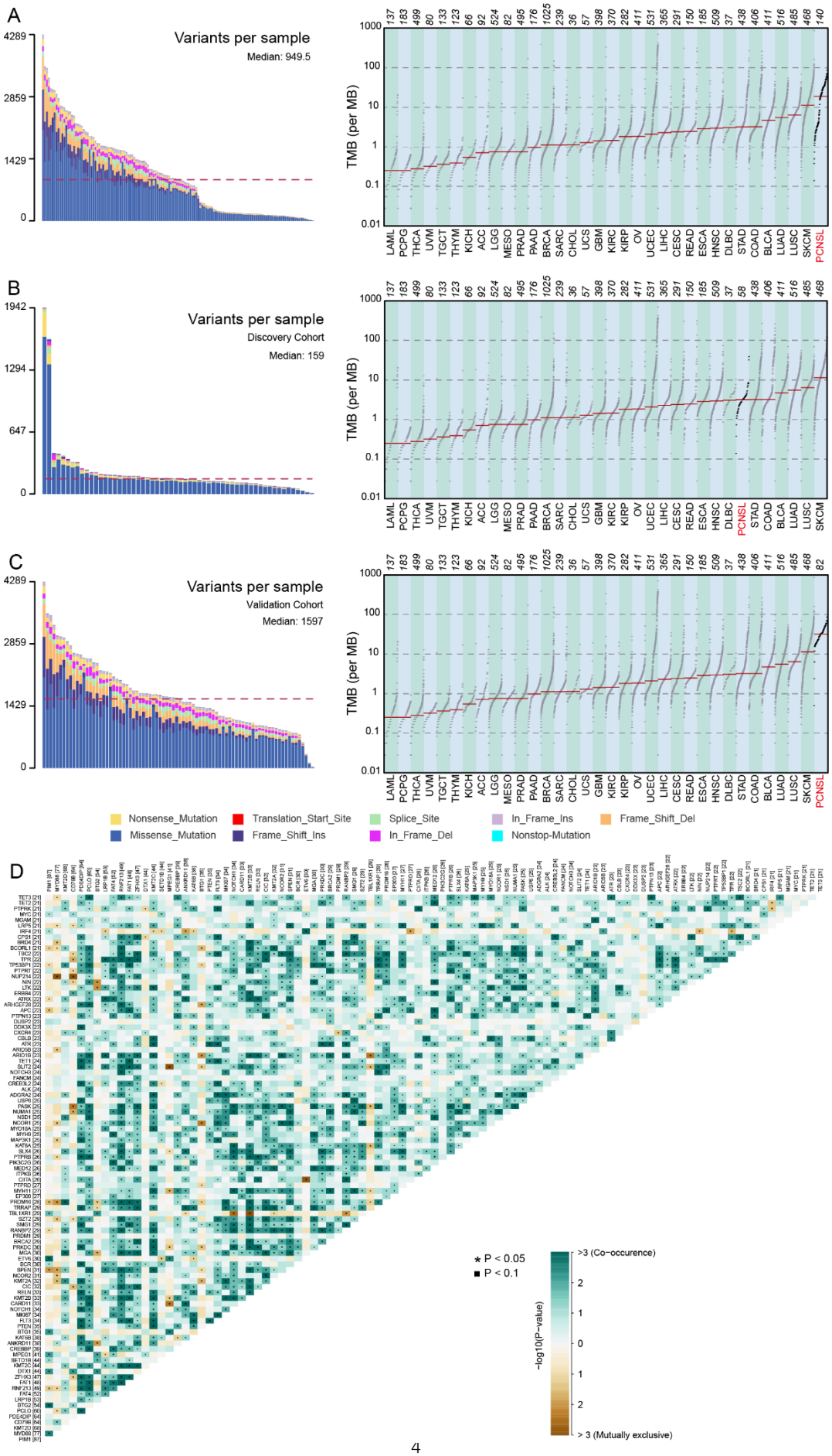
A
Variants per sample
Median: 949.5
4289
2859
1429
0
TMB (per MB)
1000
100
10
1
0.1
0.01
LAML PCPG THCA UVM TGCT THYM KICH ACC LGG MESO PRAD PAAD BRCA SARC CHOL UCS GBM KIRC KIRP OV UCEC LIHC CESC READ ESCA HNSC DLBC STAD COAD BLCA LUAD LUSC SKCM PCNSL
B
Variants per sample
Discovery Cohort
Median: 159
1942
1294
647
0
LAML PCPG THCA UVM TGCT THYM KICH ACC LGG MESO PRAD PAAD BRCA SARC CHOL UCS GBM KIRC KIRP OV UCEC LIHC CESC READ ESCA HNSC DLBC PCNSL STAD COAD BLCA LUAD LUSC SKCM
C
Variants per sample
Validation Cohort
Median: 1597
4289
2859
1429
0
LAML PCPG THCA UVM TGCT THYM KICH ACC LGG MESO PRAD PAAD BRCA SARC CHOL UCS GBM KIRC KIRP OV UCEC LIHC CESC READ ESCA HNSC DLBC STAD COAD BLCA LUAD LUSC SKCM PCNSL
Nonsense_Mutation
Missense_Mutation
Translation_Start_Site
Frame_Shift_Ins
Splice_Site
In_Frame_Del
In_Frame_Ins
Nonstop-Mutation
Frame_Shift_Del
D
* P < 0.05
■ P < 0.1
−log10(P−value)
>3 (Co−occurence)
2
1
0
1
2
> 3 (Mutually exclusive)

Figure S3. Genetic variation events and tumor mutational burden (TMB) in the 140 PCNSL samples

A: Genetic variation events in 140 PCNSL samples and the TMB of PCNSL, ranking 2nd in the TCGA database.

B: Genetic variation events in the discovery cohort of PCNSL patients (n = 58) and the TMB of PCNSL patients, ranking 5th in the TCGA database.

C: Genetic variation events in the validation cohort of PCNSL patients (n = 82) and the TMB of PCNSL patients, ranking 1st in the TCGA database.

D: The mutually exclusive or co-occurrence relationships of these genes.

Related to Figure 1.

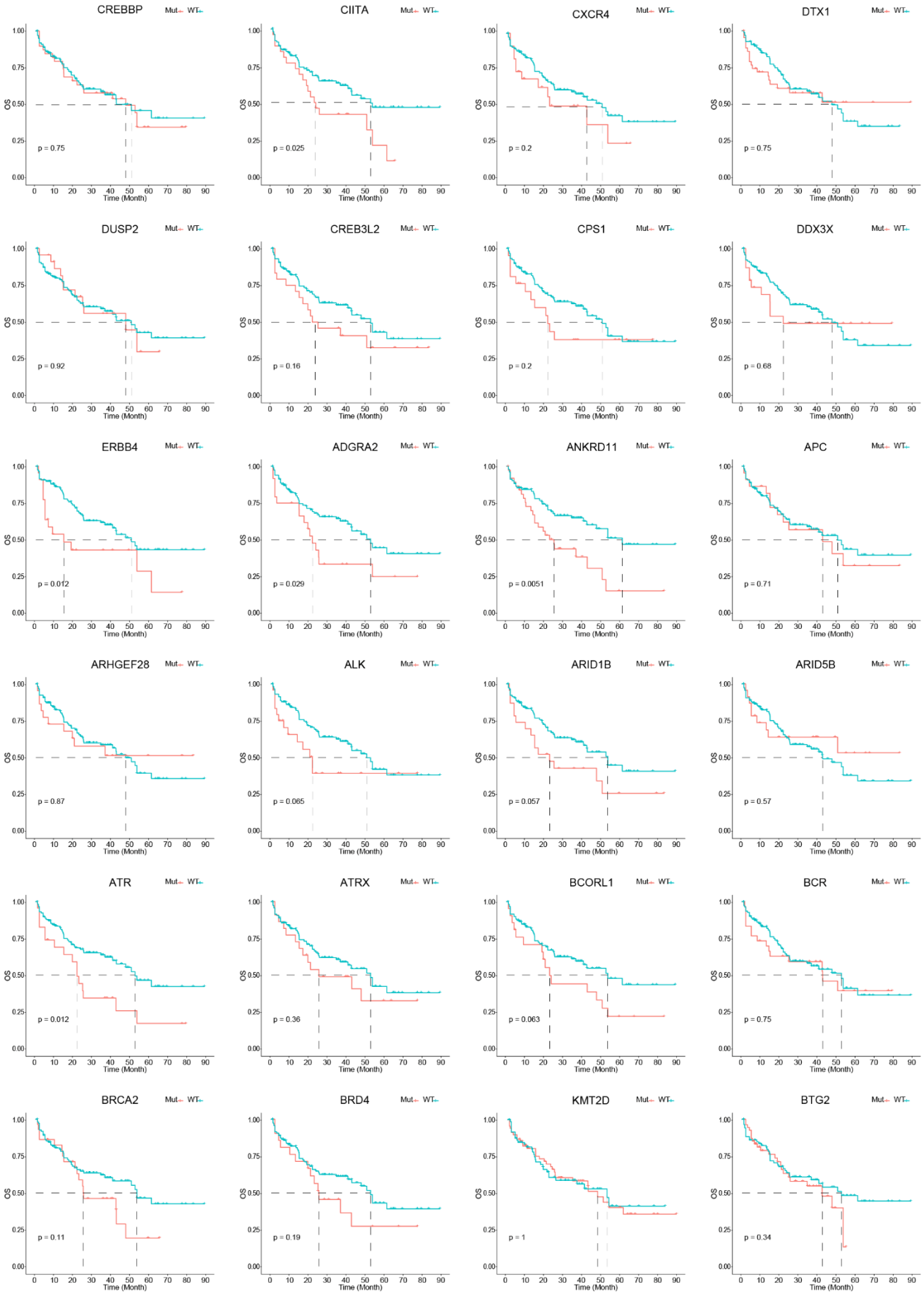
CREBBP
p = 0.75
CIITA
p = 0.025
CXCR4
p = 0.2
DTX1
p = 0.75
DUSP2
p = 0.92
CREB3L2
p = 0.16
CPS1
p = 0.2
DDX3X
p = 0.68
ERBB4
p = 0.012
ADGRA2
p = 0.029
ANKRD11
p = 0.0051
APC
p = 0.71
ARHGEF28
p = 0.87
ALK
p = 0.065
ARID1B
p = 0.057
ARID5B
p = 0.57
ATR
p = 0.012
ATRX
p = 0.36
BCORL1
p = 0.063
BCR
p = 0.75
BRCA2
p = 0.11
BRD4
p = 0.19
KMT2D
p = 1
BTG2
p = 0.34
Mut
WT
OS
Time (Month)

26

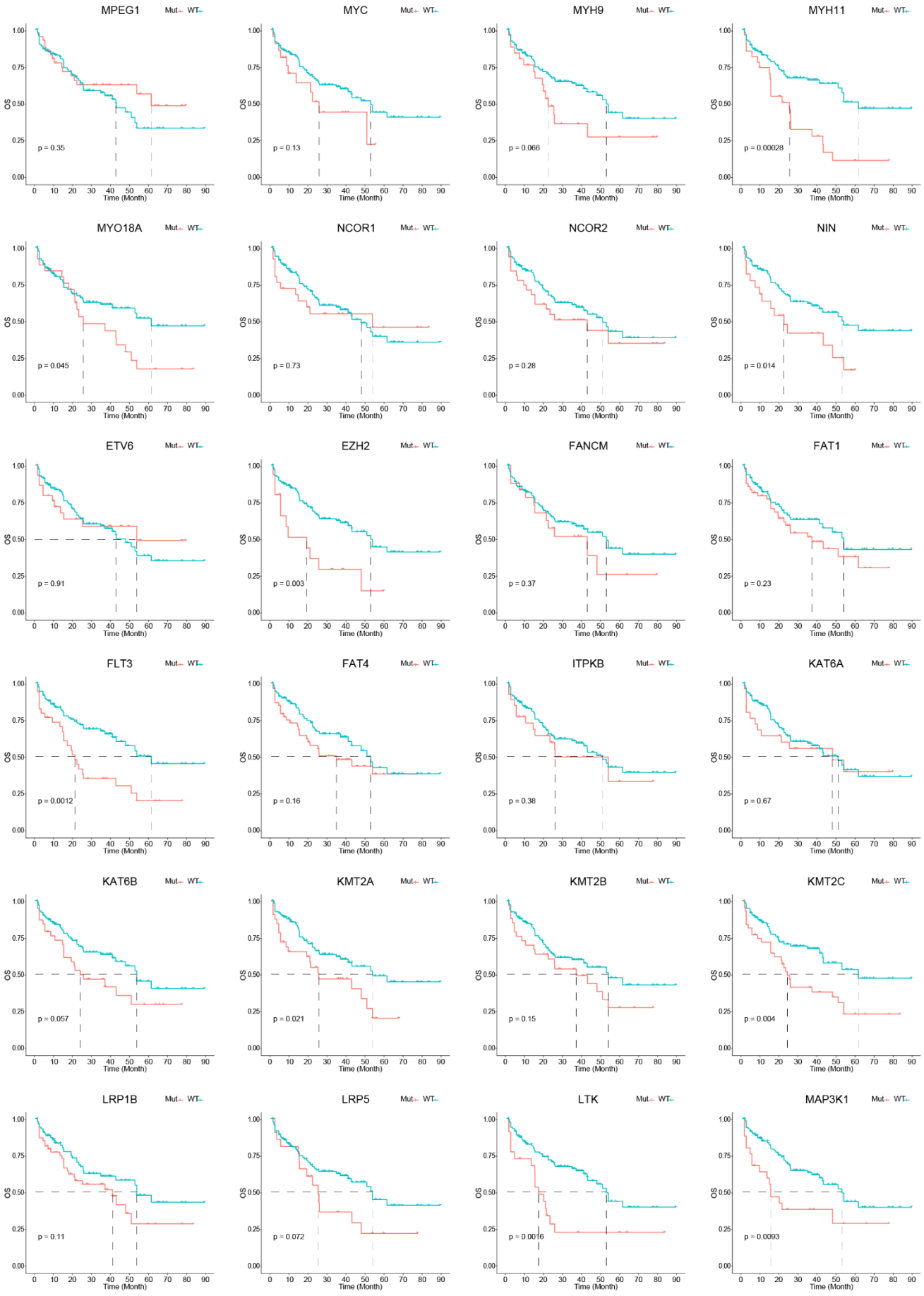
MPEG1 Mut WT p = 0.35
MYC Mut WT p = 0.13
MYH9 Mut WT p = 0.066
MYH11 Mut WT p = 0.00028
MYO18A Mut WT p = 0.045
NCOR1 Mut WT p = 0.73
NCOR2 Mut WT p = 0.28
NIN Mut WT p = 0.014
ETV6 Mut WT p = 0.91
EZH2 Mut WT p = 0.003
FANCM Mut WT p = 0.37
FAT1 Mut WT p = 0.23
FLT3 Mut WT p = 0.0012
FAT4 Mut WT p = 0.16
ITPKB Mut WT p = 0.38
KAT6A Mut WT p = 0.67
KAT6B Mut WT p = 0.057
KMT2A Mut WT p = 0.021
KMT2B Mut WT p = 0.15
KMT2C Mut WT p = 0.004
LRP1B Mut WT p = 0.11
LRP5 Mut WT p = 0.072
LTK Mut WT p = 0.0016
MAP3K1 Mut WT p = 0.0093
OS
Time (Month)

27

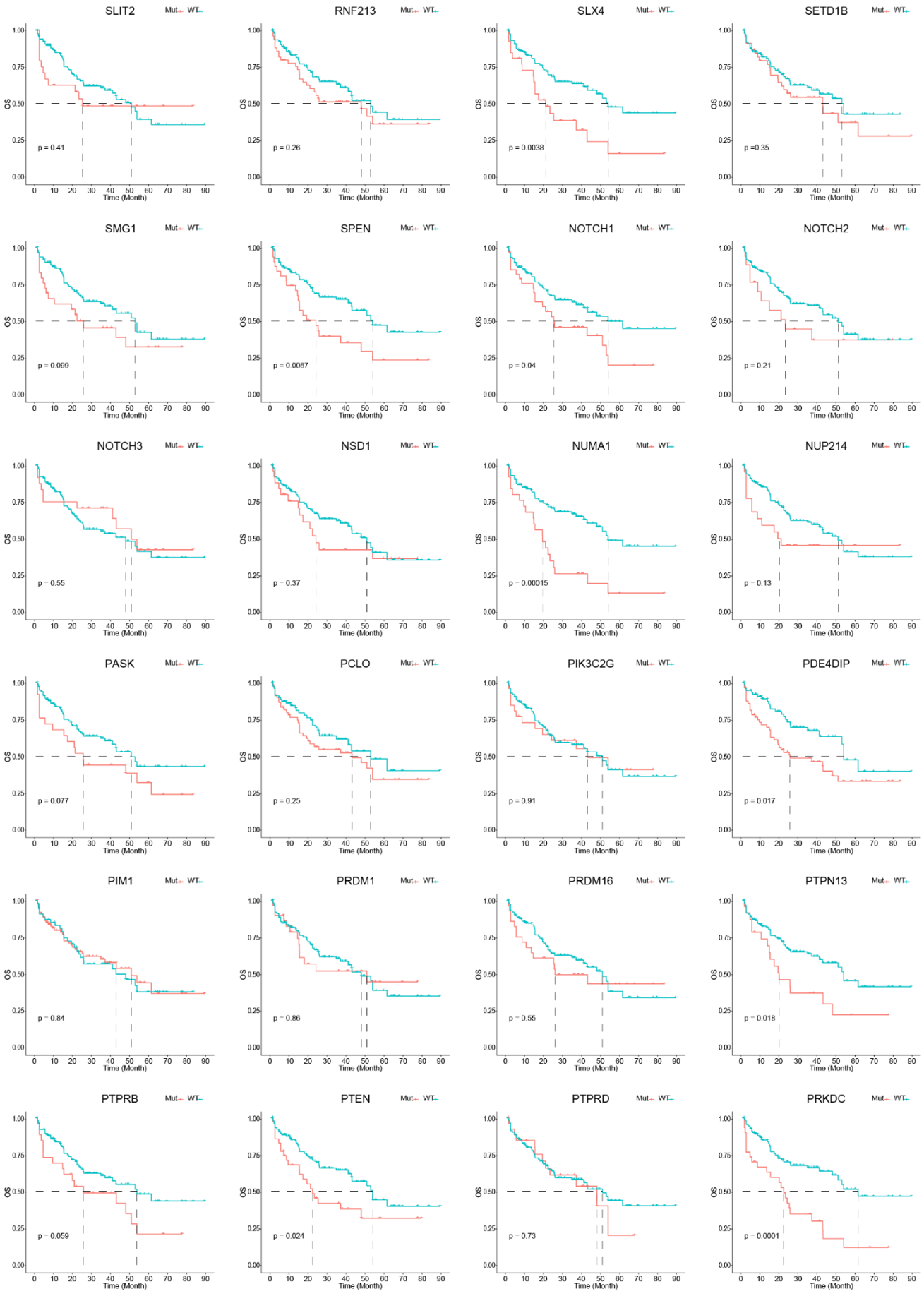
SLIT2 Mut WT p = 0.41
RNF213 Mut WT p = 0.26
SLX4 Mut WT p = 0.0038
SETD1B Mut WT p =0.35
SMG1 Mut WT p = 0.099
SPEN Mut WT p = 0.0087
NOTCH1 Mut WT p = 0.04
NOTCH2 Mut WT p = 0.21
NOTCH3 Mut WT p = 0.55
NSD1 Mut WT p = 0.37
NUMA1 Mut WT p = 0.00015
NUP214 Mut WT p = 0.13
PASK Mut WT p = 0.077
PCLO Mut WT p = 0.25
PIK3C2G Mut WT p = 0.91
PDE4DIP Mut WT p = 0.017
PIM1 Mut WT p = 0.84
PRDM1 Mut WT p = 0.86
PRDM16 Mut WT p = 0.55
PTPN13 Mut WT p = 0.018
PTPRB Mut WT p = 0.059
PTEN Mut WT p = 0.024
PTPRD Mut WT p = 0.73
PRKDC Mut WT p = 0.0001
OS
Time (Month)

28

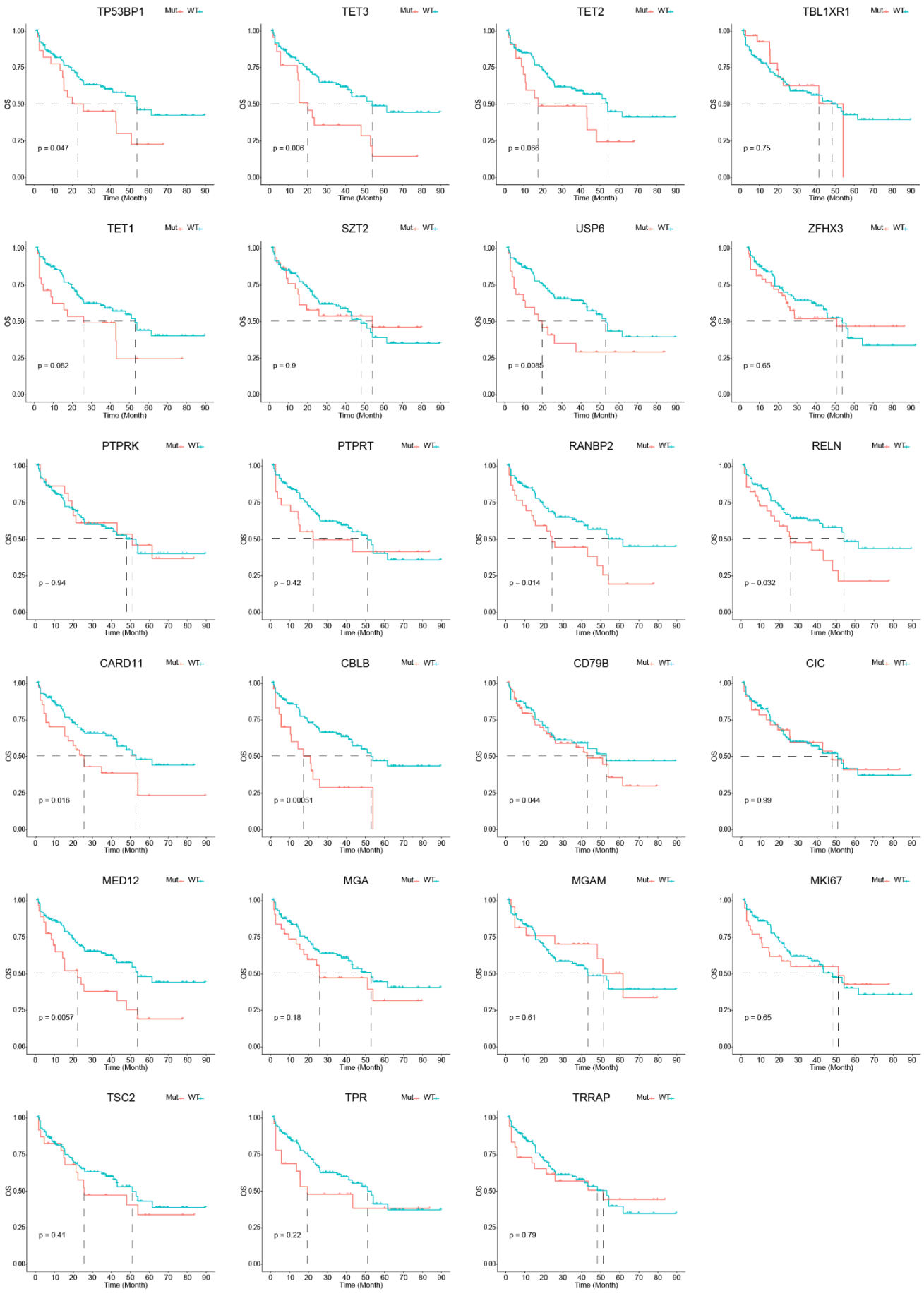
TP53BP1 Mut WT p = 0.047
TET3 Mut WT p = 0.006
TET2 Mut WT p = 0.066
TBL1XR1 Mut WT p = 0.75
TET1 Mut WT p = 0.082
SZT2 Mut WT p = 0.9
USP6 Mut WT p = 0.0085
ZFHX3 Mut WT p = 0.65
PTPRK Mut WT p = 0.94
PTPRT Mut WT p = 0.42
RANBP2 Mut WT p = 0.014
RELN Mut WT p = 0.032
CARD11 Mut WT p = 0.016
CBLB Mut WT p = 0.00051
CD79B Mut WT p = 0.044
CIC Mut WT p = 0.99
MED12 Mut WT p = 0.0057
MGA Mut WT p = 0.18
MGAM Mut WT p = 0.61
MKI67 Mut WT p = 0.65
TSC2 Mut WT p = 0.41
TPR Mut WT p = 0.22
TRRAP Mut WT p = 0.79
OS
Time (Month)

29

Figure S4. Kaplan–Meier estimates of overall survival associated with candidate cancer genes with mutation frequencies exceeding 10% and the NOTCH1, NOTCH2, and EZH2 genes.

Related to Figure 1.

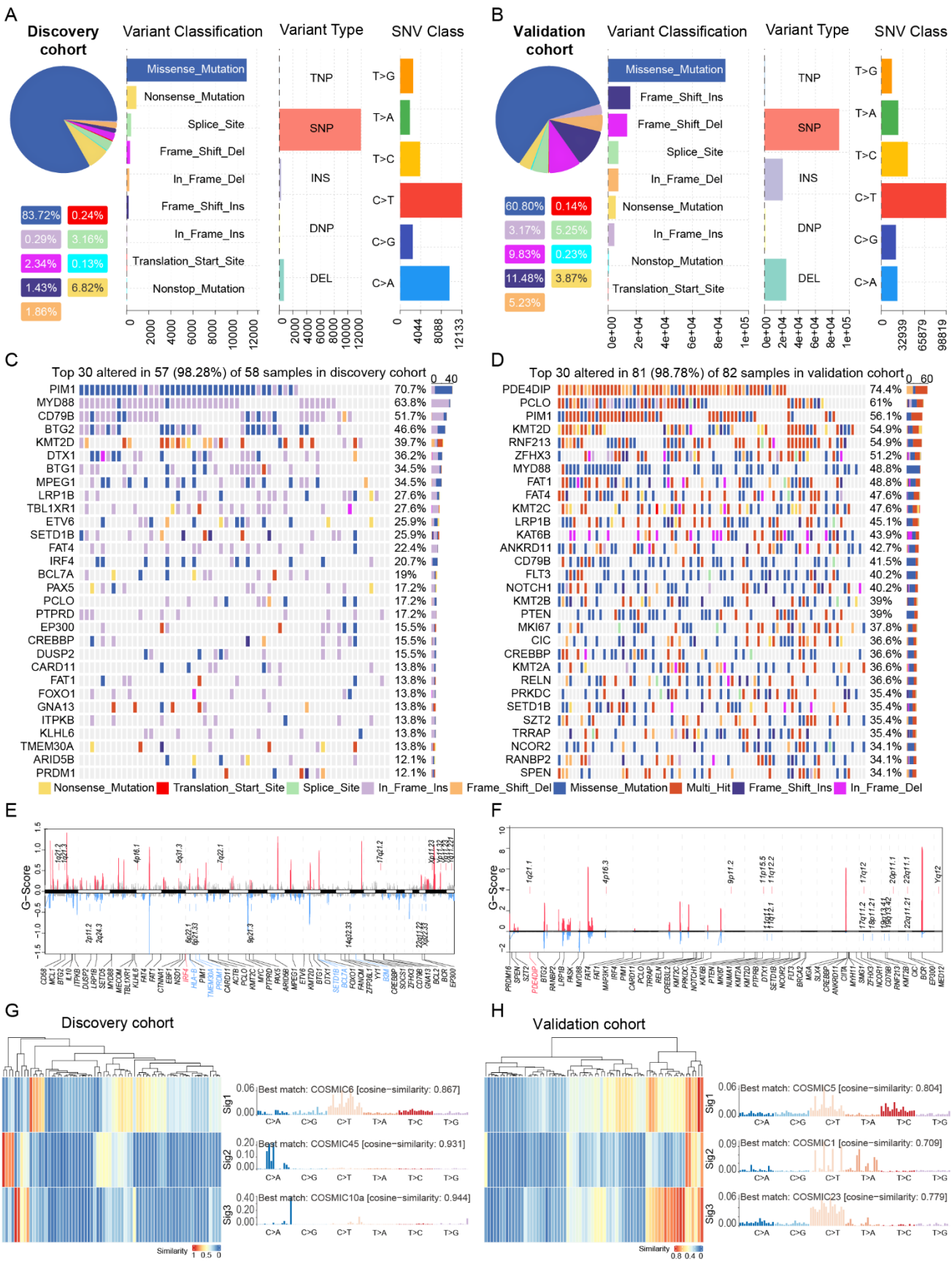

Figure S5. Mutation Profiles and Signatures of the Discovery and Validation Cohorts

A: Variant classification, type, and single-nucleotide variation (SNV) class in the discovery cohort of PCNSL patients (n = 58).

B: Variant classification, type, and single-nucleotide variation (SNV) class in the validation cohort of PCNSL patients (n = 82).

C: Number and frequency of recurrent mutations, along with a gene–sample matrix of recurrently mutated genes, ranked by mutation frequency in the discovery cohort of PCNSL patients (n = 58).

D: Number and frequency of recurrent mutations, along with a gene–sample matrix of recurrently mutated genes, ranked by mutation frequency in the validation cohort of PCNSL patients (n = 82).

E: GISTIC2.0 results of significant recurrent focal amplifications (red) and deletions (blue). Genes affected by each focal event are annotated in the discovery cohort (n = 58). X-axis: plot of chromosomes; Y-axis: G score.

F: GISTIC2.0 results of significant recurrent focal amplifications (red) and deletions (blue). Genes affected by each focal event are annotated in the validation cohort (n = 82). X-axis: plot of chromosomes; Y-axis: G score.

G: The most significant contributions to the PCNSL genome in the discovery cohort (n = 58).

H: The most significant contributions to the PCNSL genome in the validation cohort (n = 82).

Related to Figure 2.

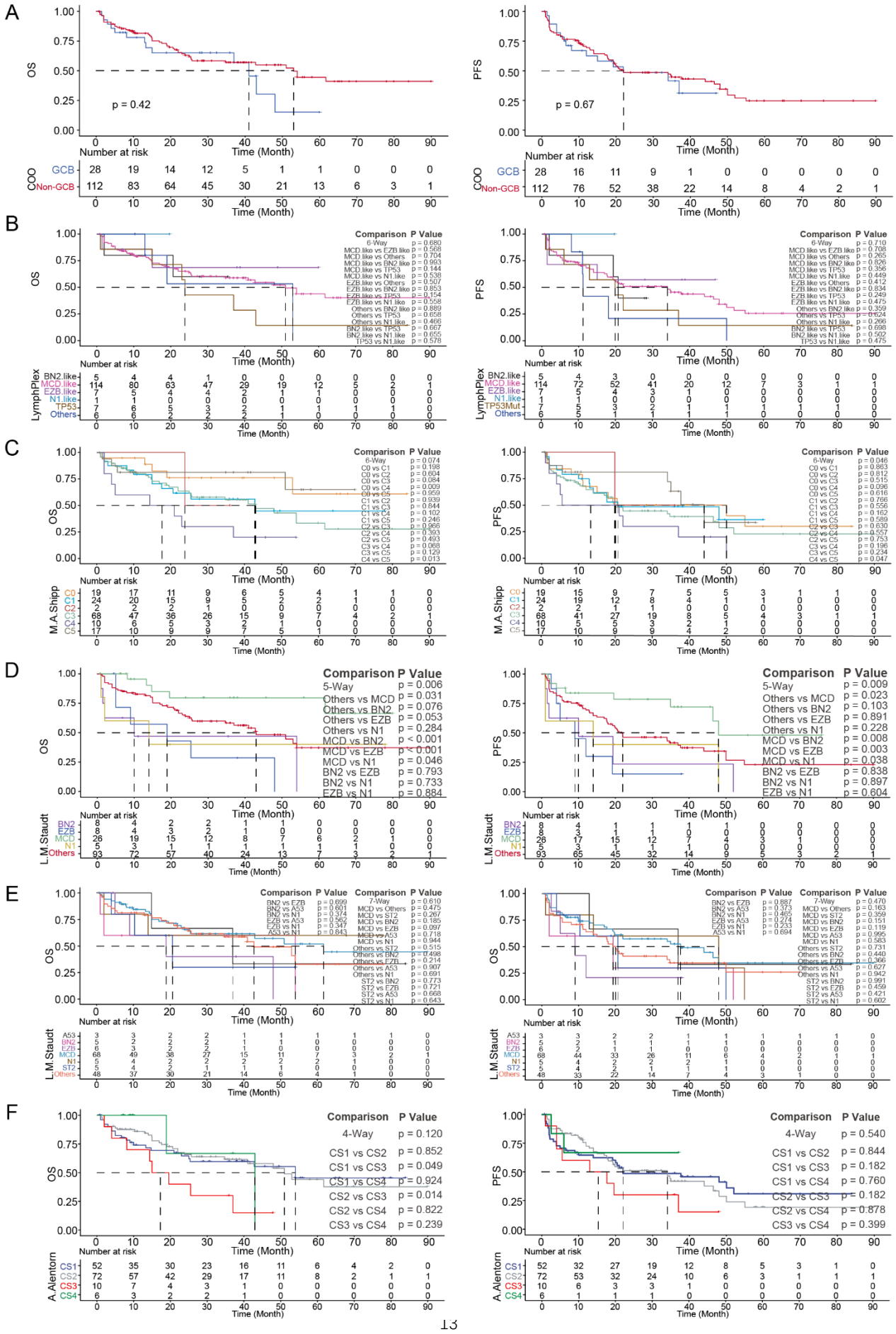
A
OS
p = 0.42
Number at risk
COO
GCB 28 19 14 12 5 1 1 0 0 0
Non-GCB 112 83 64 45 30 21 13 6 3 1
Time (Month)
PFS
p = 0.67
Number at risk
COO
GCB 28 16 11 9 1 0 0 0 0 0
Non-GCB 112 76 52 38 22 14 8 4 2 1
Time (Month)
B
OS
Comparison P Value
6-Way p = 0.680
MCD.like vs EZB.like p = 0.568
MCD.like vs Others p = 0.704
MCD.like vs BN2.like p = 0.993
MCD.like vs TP53 p = 0.144
MCD.like vs N1.like p = 0.538
EZB.like vs Others p = 0.507
EZB.like vs BN2.like p = 0.853
EZB.like vs TP53 p = 0.154
EZB.like vs N1.like p = 0.558
Others vs BN2.like p = 0.889
Others vs TP53 p = 0.658
Others vs N1.like p = 0.466
BN2.like vs TP53 p = 0.667
BN2.like vs N1.like p = 0.655
TP53 vs N1.like p = 0.578
Number at risk
LymphPlex
BN2.like 5 4 4 1 0 0 0 0 0 0
MCD.like 114 80 63 47 29 19 12 5 2 1
EZB.like 7 5 4 4 2 1 1 0 0 0
N1.like 1 1 0 0 0 0 0 0 0 0
TP53 7 6 5 3 2 1 1 1 1 0
Others 6 6 2 2 1 0 0 0 0 0
Time (Month)
PFS
Comparison P Value
6-Way p = 0.710
MCD.like vs EZB.like p = 0.708
MCD.like vs Others p = 0.265
MCD.like vs BN2.like p = 0.826
MCD.like vs TP53 p = 0.356
MCD.like vs N1.like p = 0.449
EZB.like vs Others p = 0.412
EZB.like vs BN2.like p = 0.834
EZB.like vs TP53 p = 0.249
EZB.like vs N1.like p = 0.475
Others vs BN2.like p = 0.359
Others vs TP53 p = 0.624
Others vs N1.like p = 0.266
BN2.like vs TP53 p = 0.698
BN2.like vs N1.like p = 0.502
TP53 vs N1.like p = 0.475
Number at risk
LymphPlex
BN2.like 5 4 3 0 0 0 0 0 0 0
MCD.like 114 72 52 41 20 12 7 3 1 1
EZB.like 7 5 4 3 1 0 0 0 0 0
N1.like 1 1 0 0 0 0 0 0 0 0
TP53Mut 7 5 3 2 1 1 1 1 1 0
Others 6 5 1 1 1 1 0 0 0 0
Time (Month)
C
OS
Comparison P Value
6-Way p = 0.074
C0 vs C1 p = 0.198
C0 vs C2 p = 0.604
C0 vs C3 p = 0.084
C0 vs C4 p = 0.009
C0 vs C5 p = 0.959
C1 vs C2 p = 0.939
C1 vs C3 p = 0.844
C1 vs C4 p = 0.102
C1 vs C5 p = 0.246
C2 vs C3 p = 0.966
C2 vs C4 p = 0.393
C2 vs C5 p = 0.493
C3 vs C4 p = 0.068
C3 vs C5 p = 0.129
C4 vs C5 p = 0.013
Number at risk
M.A.Shipp
C0 19 17 11 9 6 5 4 1 1 0
C1 24 20 15 9 5 2 2 1 0 0
C2 2 2 2 1 0 0 0 0 0 0
C3 68 47 36 26 15 9 7 4 2 1
C4 10 6 5 3 2 1 0 0 0 0
C5 17 10 9 9 7 5 1 0 0 0
Time (Month)
PFS
Comparison P Value
6-Way p = 0.046
C0 vs C1 p = 0.863
C0 vs C2 p = 0.812
C0 vs C3 p = 0.515
C0 vs C4 p = 0.096
C0 vs C5 p = 0.616
C1 vs C2 p = 0.766
C1 vs C3 p = 0.556
C1 vs C4 p = 0.162
C1 vs C5 p = 0.589
C2 vs C3 p = 0.630
C2 vs C4 p = 0.557
C2 vs C5 p = 0.753
C3 vs C4 p = 0.196
C3 vs C5 p = 0.234
C4 vs C5 p = 0.047
Number at risk
M.A.Shipp
C0 19 15 9 7 5 5 3 1 1 0
C1 24 19 12 8 4 1 1 0 0 0
C2 2 2 1 1 0 0 0 0 0 0
C3 68 41 27 19 8 5 4 3 1 1
C4 10 5 5 3 2 1 0 0 0 0
C5 17 10 9 9 4 2 0 0 0 0
Time (Month)
D
OS
Comparison P Value
5-Way p = 0.006
Others vs MCD p = 0.031
Others vs BN2 p = 0.076
Others vs EZB p = 0.053
Others vs N1 p = 0.284
MCD vs BN2 p < 0.001
MCD vs EZB p < 0.001
MCD vs N1 p = 0.046
BN2 vs EZB p = 0.793
BN2 vs N1 p = 0.733
EZB vs N1 p = 0.884
Number at risk
L.M.Staudt
BN2 8 4 2 2 1 1 0 0 0 0
EZB 8 4 3 2 1 0 0 0 0 0
MCD 26 19 15 12 8 7 6 2 1 0
N1 5 3 1 1 1 1 1 1 0 0
Others 93 72 57 40 24 13 7 3 2 1
Time (Month)
PFS
Comparison P Value
5-Way p = 0.009
Others vs MCD p = 0.023
Others vs BN2 p = 0.103
Others vs EZB p = 0.891
Others vs N1 p = 0.228
MCD vs BN2 p = 0.008
MCD vs EZB p = 0.003
MCD vs N1 p = 0.038
BN2 vs EZB p = 0.838
BN2 vs N1 p = 0.897
EZB vs N1 p = 0.604
Number at risk
L.M.Staudt
BN2 8 4 1 1 1 1 0 0 0 0
EZB 8 3 1 1 0 0 0 0 0 0
MCD 26 17 15 12 7 4 3 1 0 0
N1 5 3 1 1 1 0 0 0 0 0
Others 93 65 45 32 14 9 5 3 2 1
Time (Month)
E
OS
Comparison P Value
BN2 vs EZB p = 0.899
BN2 vs A53 p = 0.601
BN2 vs N1 p = 0.374
EZB vs A53 p = 0.562
EZB vs N1 p = 0.347
A53 vs N1 p = 0.843
Comparison P Value
7-Way p = 0.610
MCD vs Others p = 0.475
MCD vs ST2 p = 0.267
MCD vs BN2 p = 0.185
MCD vs EZB p = 0.097
MCD vs A53 p = 0.718
MCD vs N1 p = 0.944
Others vs ST2 p = 0.515
Others vs BN2 p = 0.498
Others vs EZB p = 0.214
Others vs A53 p = 0.907
Others vs N1 p = 0.691
ST2 vs BN2 p = 0.773
ST2 vs EZB p = 0.721
ST2 vs A53 p = 0.668
ST2 vs N1 p = 0.643
Number at risk
L.M.Staudt
A53 3 3 2 2 1 1 1 1 1 0
BN2 5 2 2 2 1 1 0 0 0 0
EZB 6 3 2 2 1 0 0 0 0 0
MCD 68 49 38 27 15 11 7 3 2 1
N1 5 4 2 2 2 2 2 1 0 0
ST2 5 4 2 1 1 1 0 0 0 0
Others 48 37 30 21 14 6 4 1 0 0
Time (Month)
OS
Comparison P Value
BN2 vs EZB p = 0.887
BN2 vs A53 p = 0.373
BN2 vs N1 p = 0.465
EZB vs A53 p = 0.274
EZB vs N1 p = 0.233
A53 vs N1 p = 0.694
Comparison P Value
7-Way p = 0.470
MCD vs Others p = 0.163
MCD vs ST2 p = 0.359
MCD vs BN2 p = 0.151
MCD vs EZB p = 0.119
MCD vs A53 p = 0.995
MCD vs N1 p = 0.583
Others vs ST2 p = 0.731
Others vs BN2 p = 0.440
Others vs EZB p = 0.366
Others vs A53 p = 0.627
Others vs N1 p = 0.942
ST2 vs BN2 p = 0.991
ST2 vs EZB p = 0.459
ST2 vs A53 p = 0.421
ST2 vs N1 p = 0.602
Number at risk
L.M.Staudt
A53 3 3 2 2 1 1 1 1 1 0
BN2 6 2 1 1 1 0 0 0 0 0
EZB 6 2 1 1 0 0 0 0 0 0
MCD 68 44 33 26 11 6 4 2 1 1
N1 5 4 2 2 1 1 0 0 0 0
ST2 5 4 2 1 1 1 0 0 0 0
Others 48 33 22 14 7 4 3 1 0 0
Time (Month)
F
OS
Comparison P Value
4-Way p = 0.120
CS1 vs CS2 p = 0.852
CS1 vs CS3 p = 0.049
CS1 vs CS4 p = 0.924
CS2 vs CS3 p = 0.014
CS2 vs CS4 p = 0.822
CS3 vs CS4 p = 0.239
Number at risk
A.Alentorn
CS1 52 35 30 23 16 11 6 4 2 0
CS2 72 57 42 29 17 11 8 2 1 1
CS3 10 7 4 3 1 0 0 0 0 0
CS4 6 3 2 2 1 0 0 0 0 0
Time (Month)
PFS
Comparison P Value
4-Way p = 0.540
CS1 vs CS2 p = 0.844
CS1 vs CS3 p = 0.182
CS1 vs CS4 p = 0.760
CS2 vs CS3 p = 0.182
CS2 vs CS4 p = 0.878
CS3 vs CS4 p = 0.399
Number at risk
A.Alentorn
CS1 52 32 27 19 12 8 5 3 1 0
CS2 72 53 32 24 10 6 3 1 1 1
CS3 10 6 3 3 1 0 0 0 0 0
CS4 6 1 1 1 0 0 0 0 0 0
Time (Month)

Figure S6. The prognostic value of published molecular subtypes for progression-free survival (PFS) and overall survival (OS) in our Chinese PCNSL cohort

A: Prognostic value of the DLBCL COO molecular subtype (GCB, non-GCB) for OS and PFS in our Chinese PCNSL cohort

B: The prognostic value of DLBCL LymphPlex molecular subtypes (BN2, MCD, EZB, N1, TP53, and others) for OS and PFS in our Chinese PCNSL cohort

C: The prognostic value of M.A. Shipp's team's DLBCL molecular subtypes (C0, C1, C2, C3, C4, and C5) for OS and PFS in our Chinese PCNSL cohort

D: The prognostic value of L.M. Staudt's team's DLBCL molecular subtypes (BN2, EZB, MCD, N1, and others) for OS and PFS in our Chinese PCNSL cohort

E: The prognostic value of L.M. Staudt's DLBCL molecular subtypes (A53, BN2, EZB, MCD, N1, ST2, and others) for OS and PFS in our Chinese PCNSL cohort.

F: Prognostic value of A. Alentorn team's PCNSL molecular subtypes (CS1, CS2, CS3, and CS4) for OS and PFS in our Chinese PCNSL cohort

Related to Figure 3.

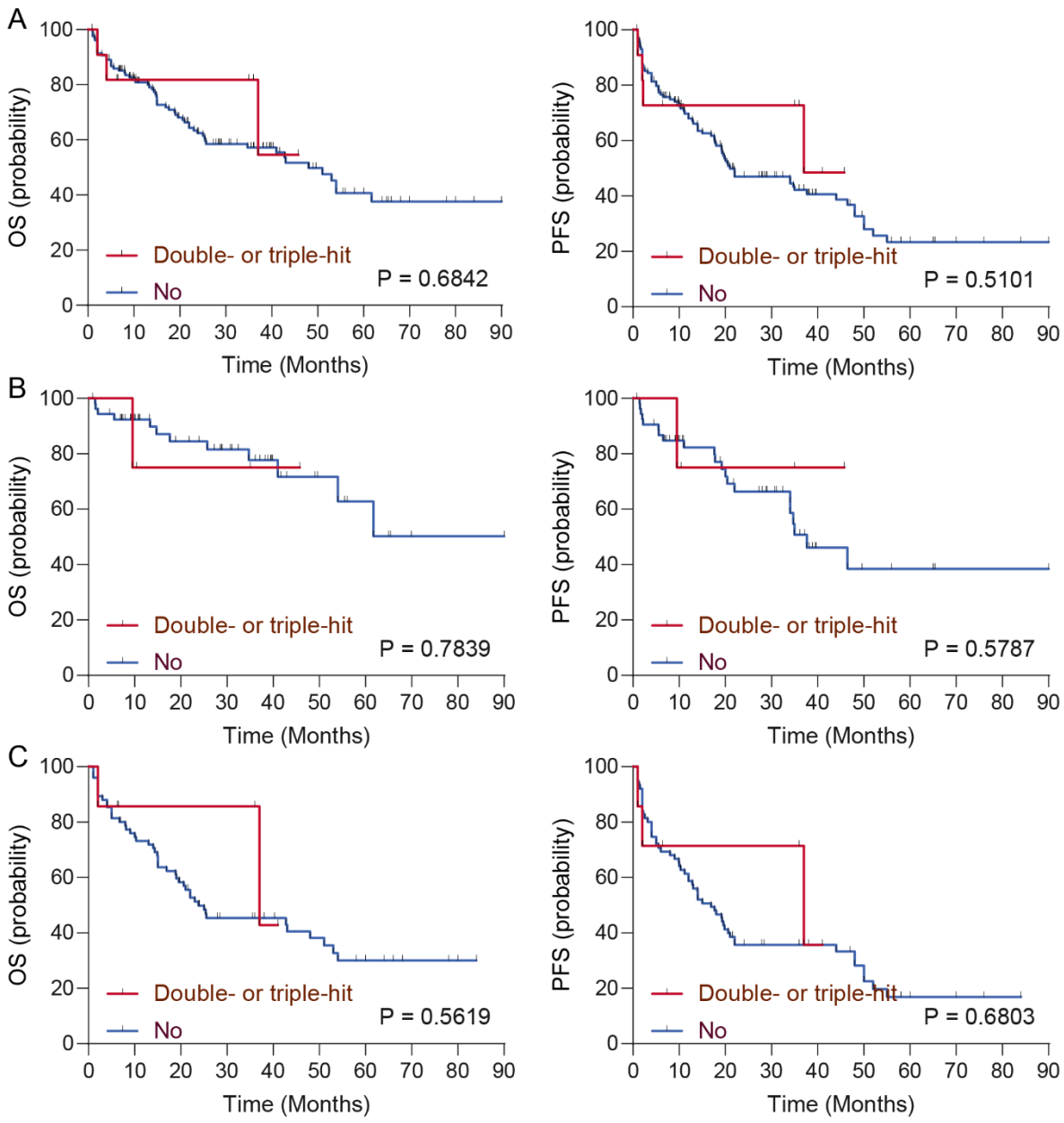

Figure S7. The prognostic value of the double-hit gene expression signature subtypes for progression-free survival (PFS) and overall survival (OS) in our Chinese PCNSL cohort

A: The prognostic value of double-hit gene expression signature subtypes (double or triple hit vs. others) for OS and PFS in our Chinese PCNSL discovery cohort (n = 58)

B: The prognostic value of double-hit gene expression signature subtypes (double or triple hit vs. others) for OS and PFS in our Chinese PCNSL validation cohort (n = 82)

C: The prognostic value of double-hit gene expression signature subtypes (double or triple hit vs. others) for OS and PFS in our Chinese PCNSL cohort (n = 140).

Related to Figure 3.

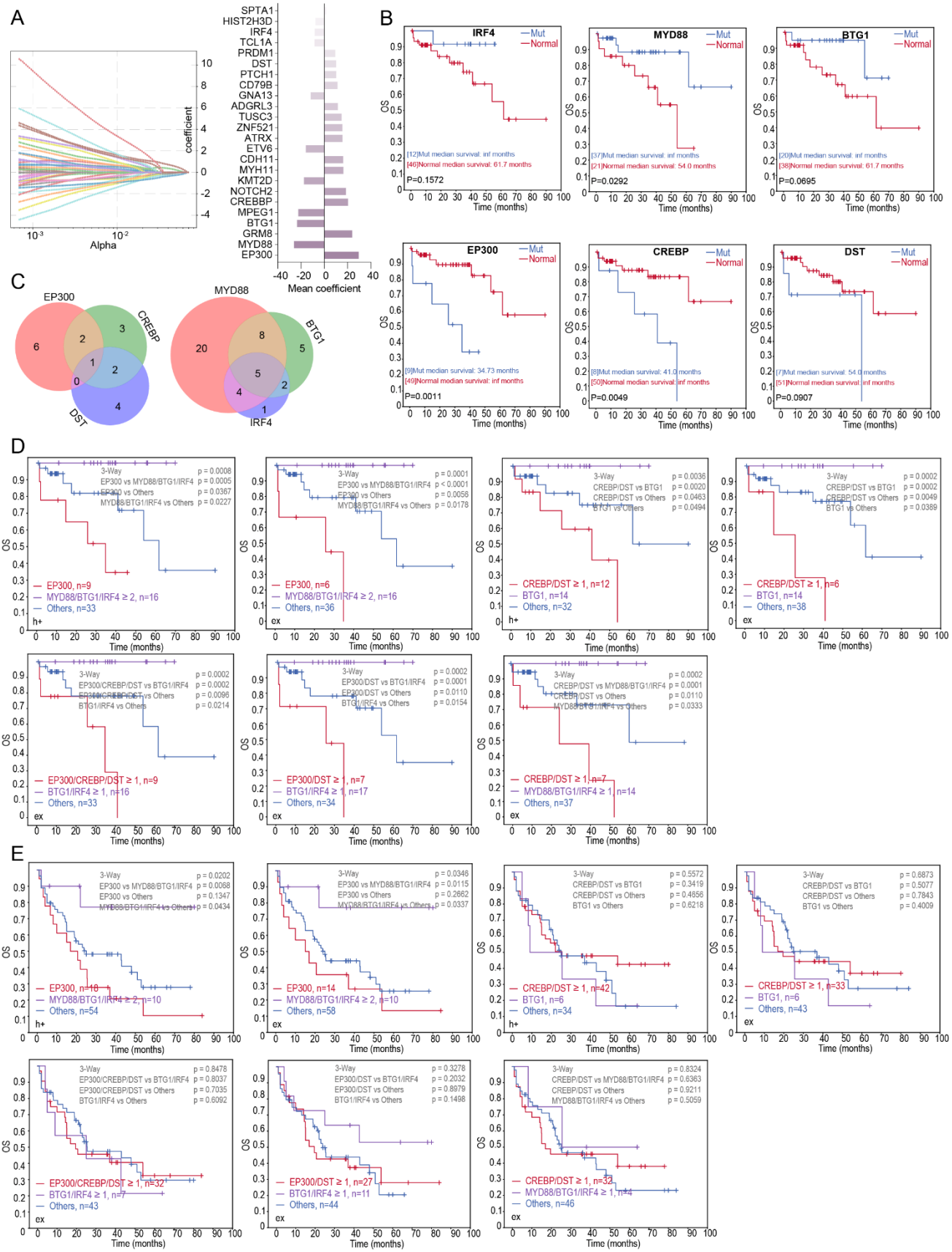

Figure S8. Schematic of the typing strategies used to identify PCNSL molecular subtypes

A: CoxNet survival analyses and least absolute shrinkage and selection operator (LASSO) regressions were employed to determine the importance score of each feature in the model, all of which were then ranked. This process was repeated 500 times, and all potential features were recorded. This is a demonstration of the aforementioned process.

B: Kaplan–Meier (K–M) analyses of the 6 identified features were conducted.

C: Venn diagram illustrating how these 6 features were randomly combined to form three types.

D: Seven candidate molecular subtype combinations were identified in the discovery cohort.

E: Seven candidate molecular subtype combinations were validated in the validation cohort.

Related to Figure 4.

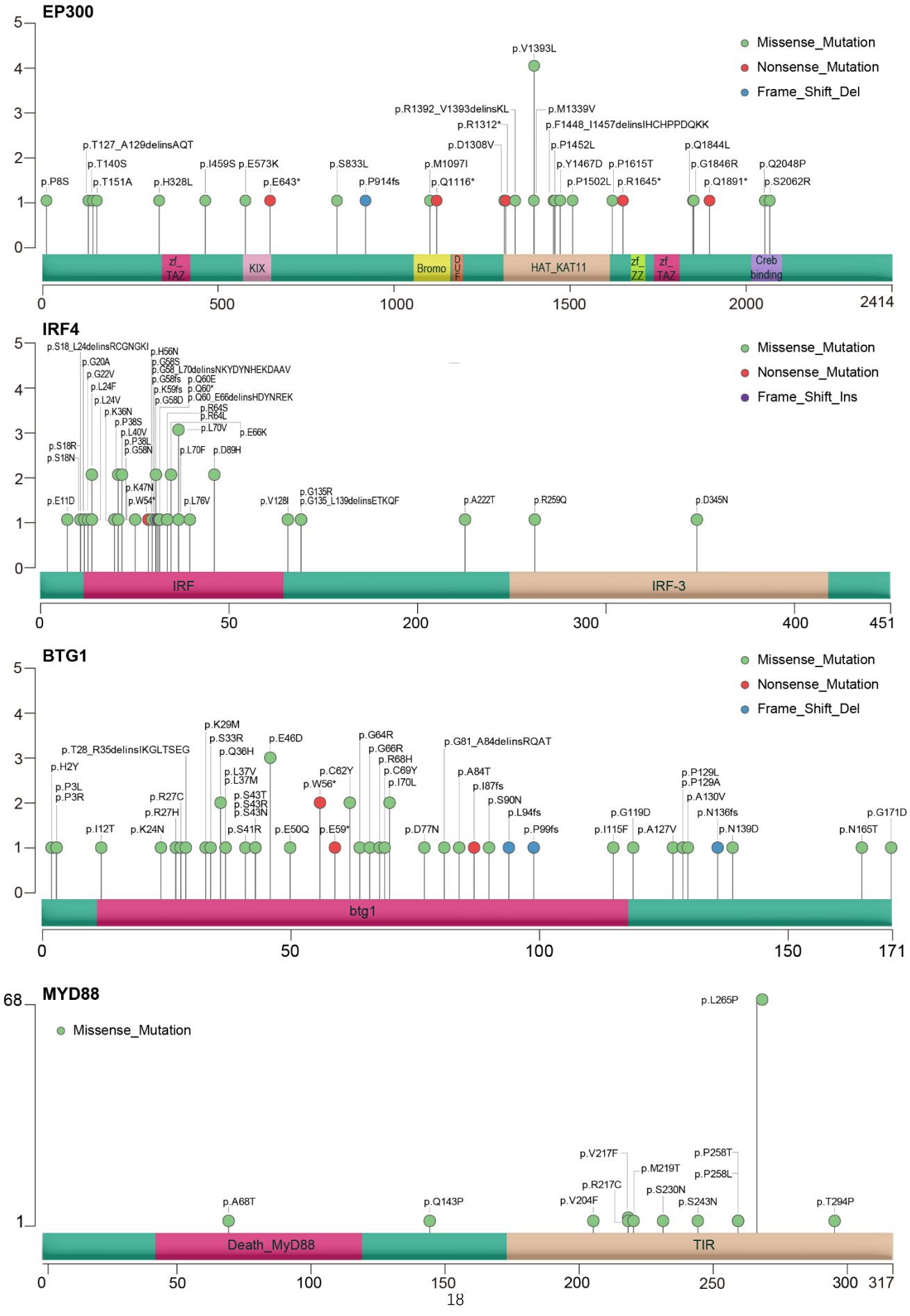
EP300
Missense_Mutation
Nonsense_Mutation
Frame_Shift_Del
p.V1393L
p.R1392_V1393delinsKL
p.M1339V
p.R1312*
p.F1448_I1457delinsIHCHPPDQKK
p.T127_A129delinsAQT
p.D1308V
p.P1452L
p.Q1844L
p.T140S
p.I459S
p.E573K
p.S833L
p.M1097I
p.Y1467D
p.P1615T
p.G1846R
p.Q2048P
p.P8S
p.T151A
p.H328L
p.E643*
p.P914fs
p.Q1116*
p.P1502L
p.R1645*
p.Q1891*
p.S2062R
zf_TAZ
KIX
Bromo
DUF
HAT_KAT11
zf_ZZ
zf_TAZ
Creb binding
0
500
1000
1500
2000
2414
IRF4
Missense_Mutation
Nonsense_Mutation
Frame_Shift_Ins
p.S18_L24delinsRCGNGKI
p.H56N
p.G20A
p.G58S
p.G58_L70delinsNKYDYNHEKDAAV
p.G22V
p.G58fs
p.Q60E
p.L24F
p.K59fs
p.Q60*
p.L24V
p.G58D
p.Q60_E66delinsHDYNREK
p.R64S
p.K36N
p.R64L
p.P38S
p.L70V
p.E66K
p.L40V
p.S18R
p.P38L
p.L70F
p.D89H
p.S18N
p.G58N
p.K47N
p.E11D
p.W54*
p.L76V
p.V128I
p.G135R
p.G135_L139delinsETKQF
p.A222T
p.R259Q
p.D345N
IRF
IRF-3
0
50
200
300
400
451
BTG1
Missense_Mutation
Nonsense_Mutation
Frame_Shift_Del
p.K29M
p.S33R
p.E46D
p.G64R
p.T28_R35delinsIKGLTSEG
p.Q36H
p.G66R
p.G81_A84delinsRQAT
p.R68H
p.H2Y
p.L37V
p.C62Y
p.C69Y
p.A84T
p.P129L
p.L37M
p.W56*
p.I70L
p.I87fs
p.P129A
p.P3L
p.S43T
p.S90N
p.A130V
p.R27C
p.S43R
p.P3R
p.L94fs
p.G119D
p.N136fs
p.G171D
p.R27H
p.S43N
p.I115F
p.A127V
p.N139D
p.I12T
p.K24N
p.S41R
p.E50Q
p.E59*
p.D77N
p.P99fs
p.N165T
btg1
0
50
100
150
171
MYD88
Missense_Mutation
p.L265P
p.V217F
p.P258T
p.M219T
p.P258L
p.R217C
p.S230N
p.A68T
p.Q143P
p.V204F
p.S243N
p.T294P
Death_MyD88
TIR
0
50
100
150
200
250
300
317

Figure S9. Mutation diagrams (Lollipop Figures) for the EP300, IRF4, BTG1, and MYD88 genes

For each gene, all nonsynonymous mutations within the functional domains of the respective protein were visualized via maftools.

Related to Figure 4.

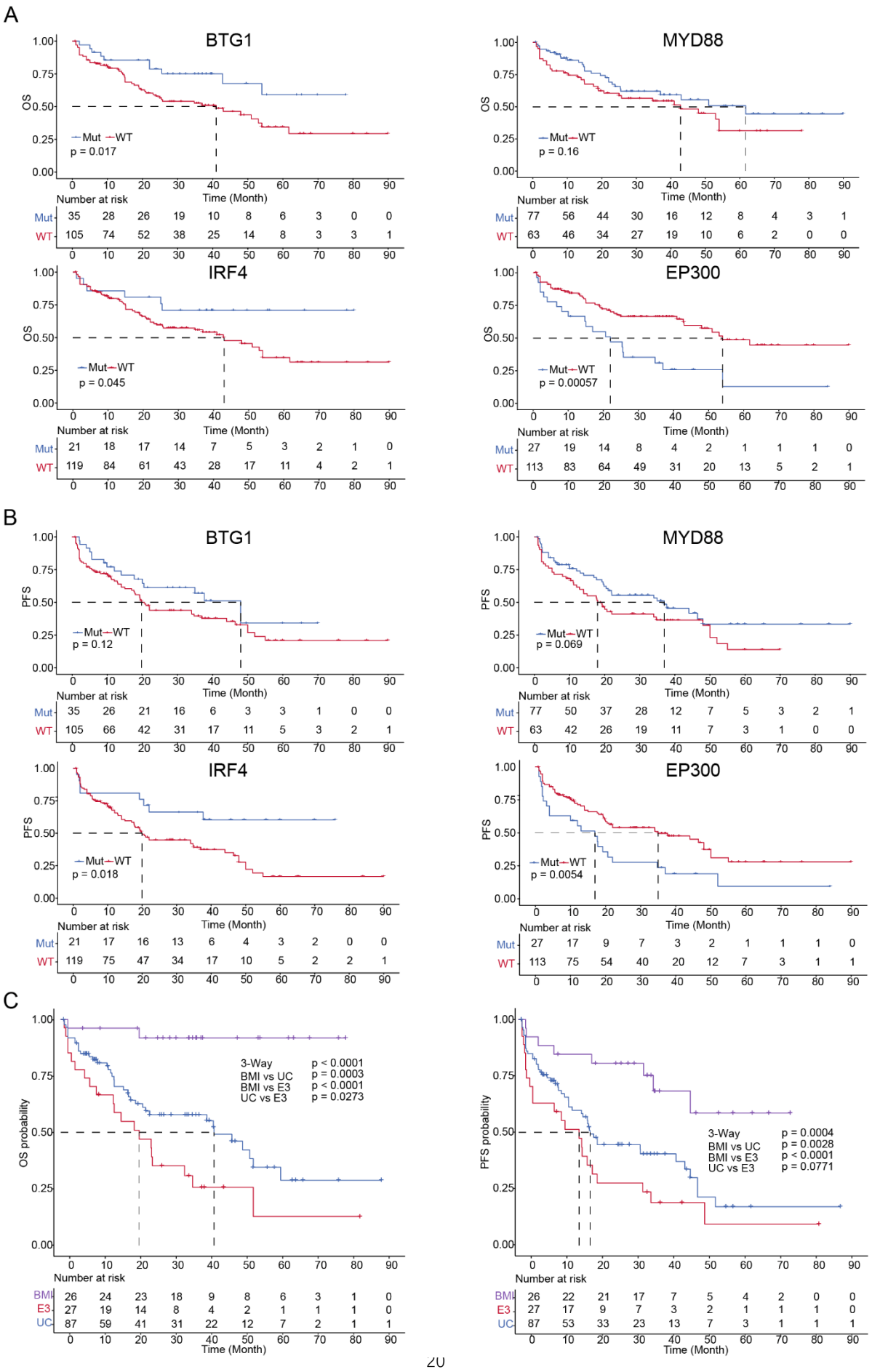
A
BTG1
OS
Mut WT
p = 0.017
Number at risk
Time (Month)
Mut 35 28 26 19 10 8 6 3 0 0
WT 105 74 52 38 25 14 8 3 3 1
MYD88
Mut WT
p = 0.16
Mut 77 56 44 30 16 12 8 4 3 1
WT 63 46 34 27 19 10 6 2 0 0
IRF4
Mut WT
p = 0.045
Mut 21 18 17 14 7 5 3 2 1 0
WT 119 84 61 43 28 17 11 4 2 1
EP300
Mut WT
p = 0.00057
Mut 27 19 14 8 4 2 1 1 1 0
WT 113 83 64 49 31 20 13 5 2 1
B
BTG1
PFS
Mut WT
p = 0.12
Mut 35 26 21 16 6 3 3 1 0 0
WT 105 66 42 31 17 11 5 3 2 1
MYD88
Mut WT
p = 0.069
Mut 77 50 37 28 12 7 5 3 2 1
WT 63 42 26 19 11 7 3 1 0 0
IRF4
Mut WT
p = 0.018
Mut 21 17 16 13 6 4 3 2 0 0
WT 119 75 47 34 17 10 5 2 2 1
EP300
Mut WT
p = 0.0054
Mut 27 17 9 7 3 2 1 1 1 0
WT 113 75 54 40 20 12 7 3 1 1
C
OS probability
3-Way p < 0.0001
BMI vs UC p = 0.0003
BMI vs E3 p < 0.0001
UC vs E3 p = 0.0273
BMI 26 24 23 18 9 8 6 3 1 0
E3 27 19 14 8 4 2 1 1 1 0
UC 87 59 41 31 22 12 7 2 1 1
PFS probability
3-Way p = 0.0004
BMI vs UC p = 0.0028
BMI vs E3 p < 0.0001
UC vs E3 p = 0.0771
BMI 26 22 21 17 7 5 4 2 0 0
E3 27 17 9 7 3 2 1 1 1 0
UC 87 53 33 23 13 7 3 1 1 1

Figure S10. Kaplan–Meier analyses of the EP300, IRF4, BTG1, and MYD88 genes and molecular subtypes

A: Prognostic value of mutations in the EP300, IRF4, BTG1, and MYD88 genes for OS.

B: Prognostic value of mutations in the EP300, IRF4, BTG1, and MYD88 genes for progression-free survival (PFS).

C: Kaplan–Meier estimates of overall survival (OS) and progression-free survival (PFS) among 140 PCNSL patients with each molecular subtype.

Related to Figure 4.

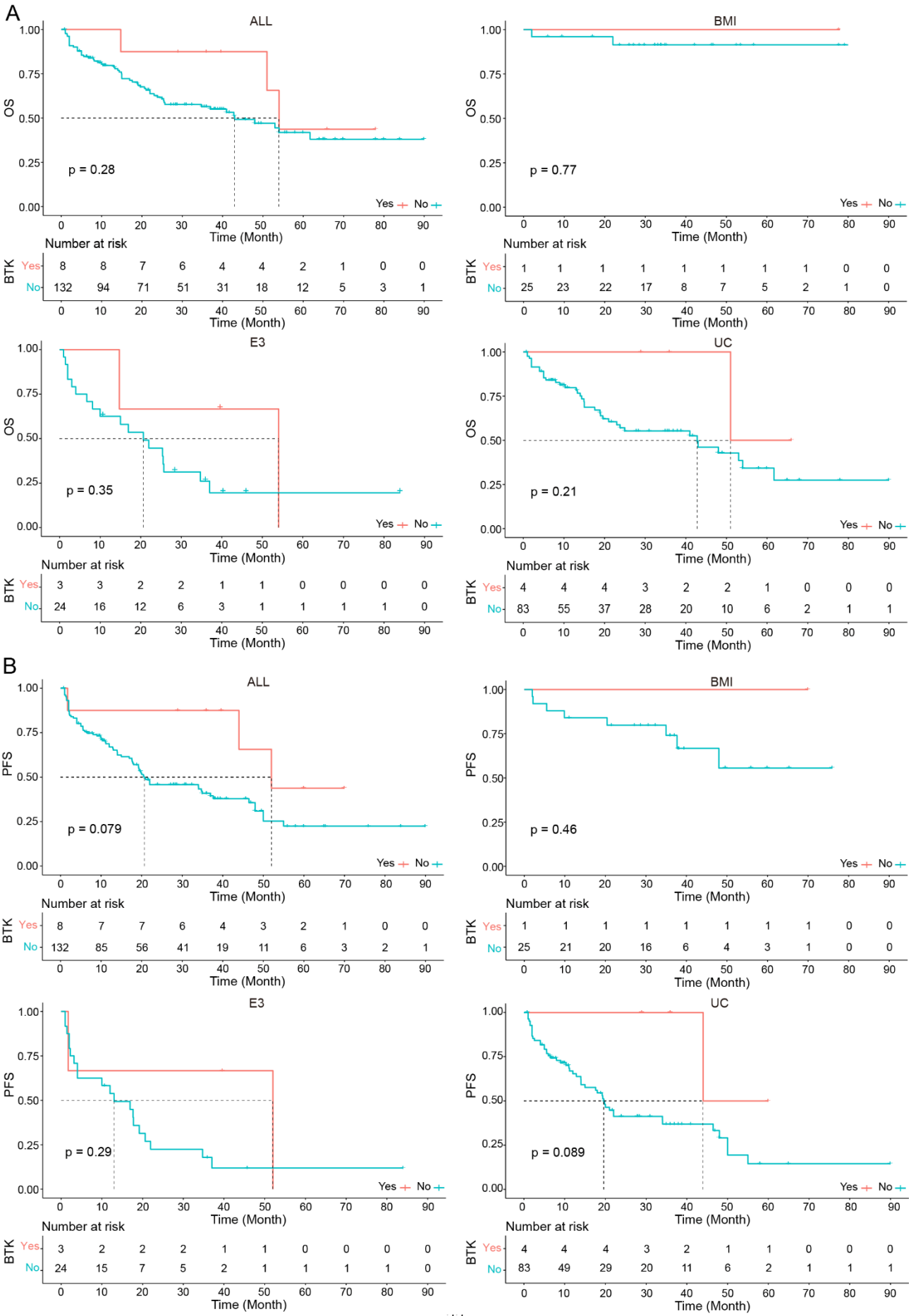
A
ALL
OS
p = 0.28
Yes No
Time (Month)
Number at risk
BTK
Yes 8 8 7 6 4 4 2 1 0 0
No 132 94 71 51 31 18 12 5 3 1
BMI
p = 0.77
Yes 1 1 1 1 1 1 1 1 0 0
No 25 23 22 17 8 7 5 2 1 0
E3
p = 0.35
Yes 3 3 2 2 1 1 0 0 0 0
No 24 16 12 6 3 1 1 1 1 0
UC
p = 0.21
Yes 4 4 4 3 2 2 1 0 0 0
No 83 55 37 28 20 10 6 2 1 1
B
ALL
PFS
p = 0.079
Yes 8 7 7 6 4 3 2 1 0 0
No 132 85 56 41 19 11 6 3 2 1
BMI
p = 0.46
Yes 1 1 1 1 1 1 1 1 0 0
No 25 21 20 16 6 4 3 1 0 0
E3
p = 0.29
Yes 3 2 2 2 1 1 0 0 0 0
No 24 15 7 5 2 1 1 1 1 0
UC
p = 0.089
Yes 4 4 4 3 2 1 1 0 0 0
No 83 49 29 20 11 6 2 1 1 1

Figure S11. Kaplan–Meier estimates of the impact of BTK inhibitor use on prognosis

A: The prognostic value of BTK inhibitor use for overall survival (OS) in all 140 PCNSL patients and patients with each molecular subtype.

B: Prognostic value of BTK inhibitor use for progression-free survival (PFS) in all 140 PCNSL patients and patients with each molecular subtype.

Related to Figure 4.

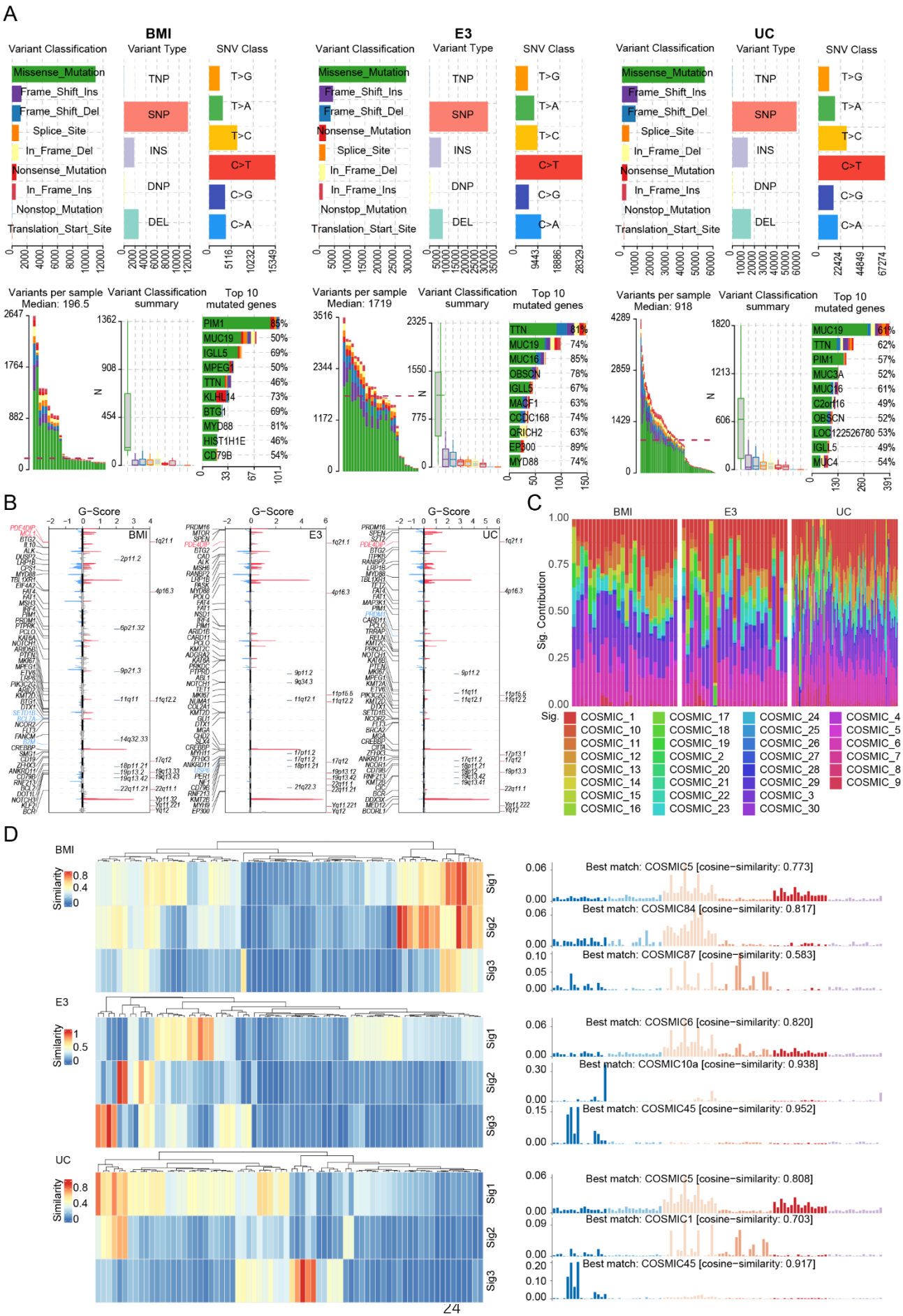
A
BMI
E3
UC
Variant Classification
Variant Type
SNV Class
Missense_Mutation
Frame_Shift_Ins
Frame_Shift_Del
Splice_Site
In_Frame_Del
Nonsense_Mutation
In_Frame_Ins
Nonstop_Mutation
Translation_Start_Site
TNP
SNP
INS
DNP
DEL
T>G
T>A
T>C
C>T
C>G
C>A
Variants per sample
Median: 196.5
Median: 1719
Median: 918
Variant Classification summary
Top 10 mutated genes
PIM1 85%
MUC19 50%
IGLL5 69%
MPEG1 50%
TTN 46%
KLHL14 73%
BTG1 69%
MYD88 81%
HIST1H1E 46%
CD79B 54%
TTN 81%
MUC19 74%
MUC16 85%
OBSCN 78%
IGLL5 67%
MACF1 63%
CCDC168 74%
ORICH2 63%
EP300 89%
MYD88 74%
MUC19 61%
TTN 62%
PIM1 57%
MUC3A 52%
MUC16 61%
C2orf16 49%
OBSCN 52%
LOC122526780 53%
IGLL5 49%
MUC4 54%
B
G-Score
BMI
E3
UC
C
Sig. Contribution
Sig.
COSMIC_1
COSMIC_10
COSMIC_11
COSMIC_12
COSMIC_13
COSMIC_14
COSMIC_15
COSMIC_16
COSMIC_17
COSMIC_18
COSMIC_19
COSMIC_2
COSMIC_20
COSMIC_21
COSMIC_22
COSMIC_23
COSMIC_24
COSMIC_25
COSMIC_26
COSMIC_27
COSMIC_28
COSMIC_29
COSMIC_3
COSMIC_30
COSMIC_4
COSMIC_5
COSMIC_6
COSMIC_7
COSMIC_8
COSMIC_9
D
Similarity
Sig1
Sig2
Sig3
Best match: COSMIC5 [cosine−similarity: 0.773]
Best match: COSMIC84 [cosine−similarity: 0.817]
Best match: COSMIC87 [cosine−similarity: 0.583]
Best match: COSMIC6 [cosine−similarity: 0.820]
Best match: COSMIC10a [cosine−similarity: 0.938]
Best match: COSMIC45 [cosine−similarity: 0.952]
Best match: COSMIC5 [cosine−similarity: 0.808]
Best match: COSMIC1 [cosine−similarity: 0.703]
Best match: COSMIC45 [cosine−similarity: 0.917]

Figure S12. Mutation profiles and signatures across the three MSs

A. Variant classification, type, and single-nucleotide variation (SNV) class across the E3, BMI, and UC subtypes.

B. GISTIC2.0 results of significant recurrent focal amplifications (red) and deletions (blue). Genes affected by each focal event are annotated. X-axis: plot of chromosomes; Y-axis: G score.

C. Contributions of mutational signatures across the E3, BMI, and UC subtypes.

D. The most significant contributions to the PCNSL genome across the E3, BMI, and UC subtypes.

Related to Figure 6.

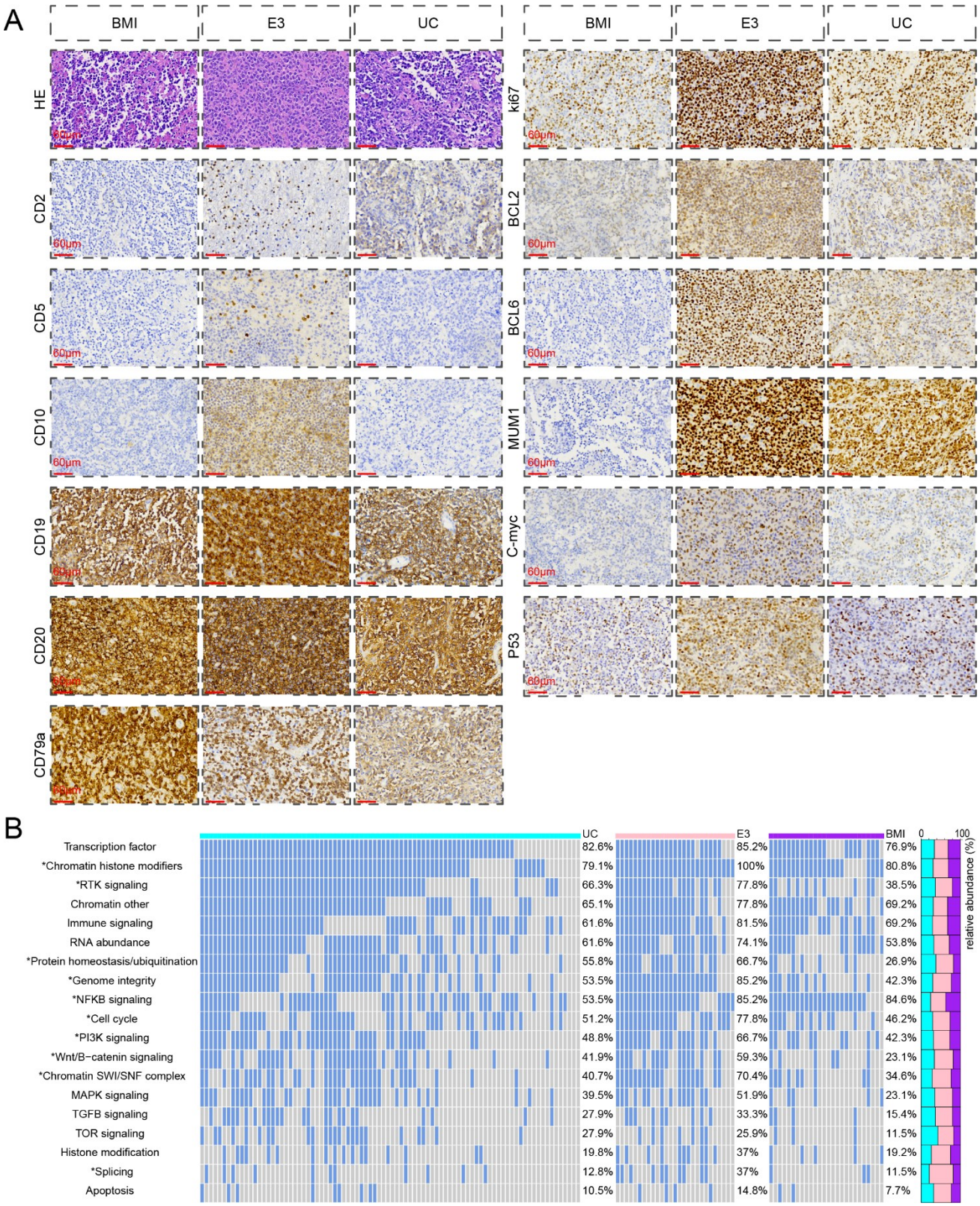

Figure S13. Hematoxylin–eosin staining and immunohistochemistry (A) for CD2, CD5, CD10, CD19, CD20, CD79a, Ki-67, BCL2, BCL6, MUM1, C-Myc, and p53, and oncogene pathways (B) in samples from different PCNSL subtypes

Related to Figure 6.

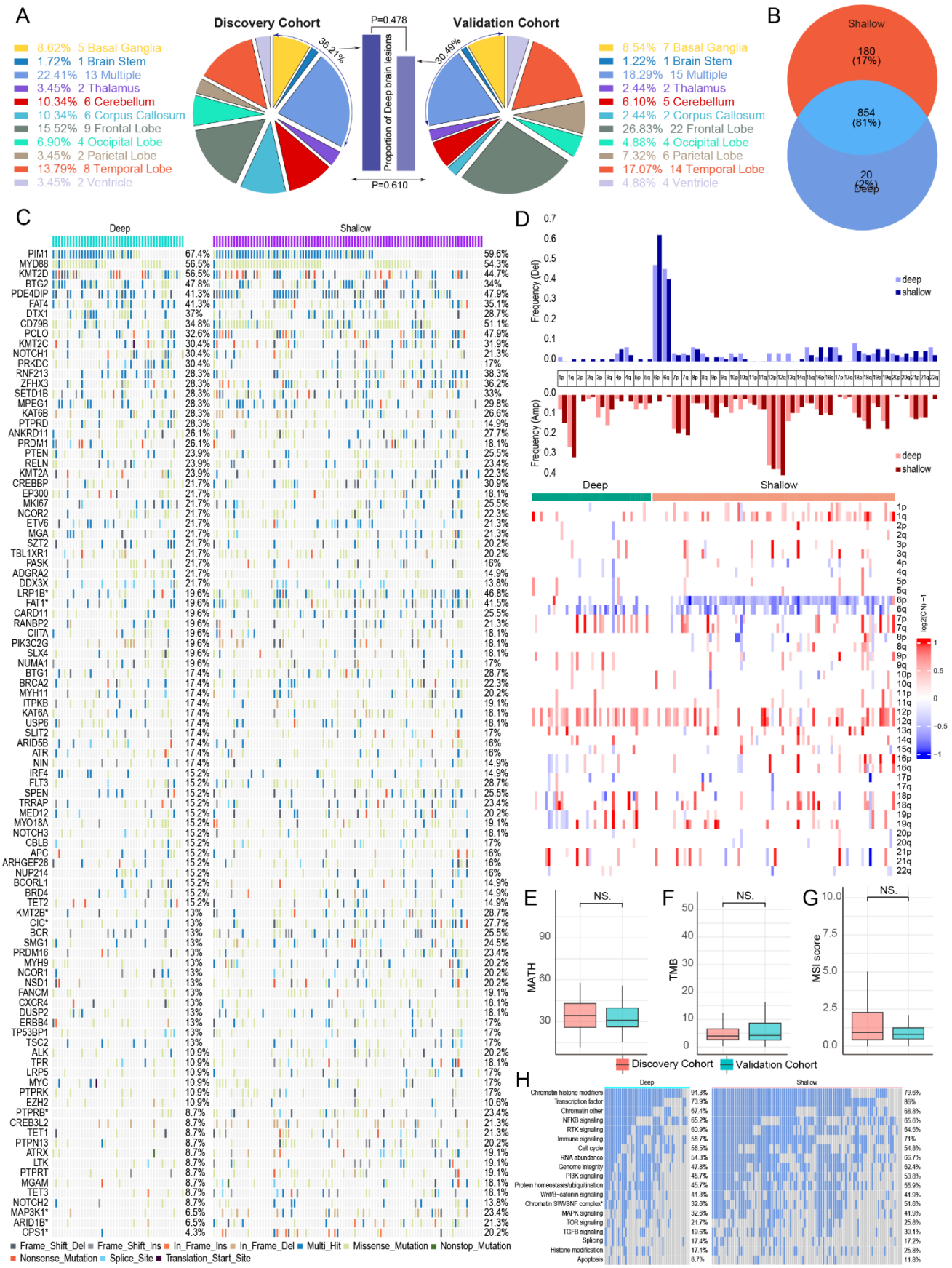

Figure S14. Mutational profiles of deep brain and shallow brain tumors in PCNSL

A: Difference in tumor sites in the discovery versus validation cohorts.

B: Venn diagram of unique and shared mutations in deep brain and shallow brain tumors.

C: The number and frequency of recurrent mutations, along with a gene-sample matrix of recurrently mutated genes in PCNSL patients between deep brain and shallow brain tumors, are presented. The relative abundance across the molecular subtypes is displayed on the right.

D: Arm-level copy number alterations between deep brain and shallow brain tumors are displayed. The frequencies of amplifications and deletions were compared.

E: The levels of mutant-allele tumor heterogeneity (MATH) were compared between deep brain and shallow brain tumors.

F: The tumor mutational burden (TMB) was compared between deep brain and shallow brain tumors.

G: The levels of microsatellite instability (MSI) were compared between deep brain and shallow brain tumors.

H: Pathways affected by oncogenes in PCNSL patients between deep brain and shallow brain tumors.

The chi-squared test and one-way ANOVA were used. $*P < 0.05$, $^{ns}P > 0.05$

Related to Figure 7.